Journal of Cancer Research and Clinical Oncology (2025) 151:93
https://doi.org/10.1007/s00432-025-06136-7

RESEARCH

^{157}Gd-DOTA-PSMA as theranostic bio-gadolinium agent for prostate cancer targeted gadolinium neutron capture therapy

Liang Xie[1] · Jialin Qin[1] · Cuiping Song[1] · Jianchun Yin[2] · Ruixue Wu[2] · Hong Chen[1,3] · Yujie Dong[3] · Nianfei Wang[4] · Lei Chen[5] · Bing Hong[6] · Ni Chen[2] · Peng Lu[6] · Fei Li[1] · Xiaoxi Pang[1,3]

Received: 22 December 2024 / Accepted: 6 February 2025 / Published online: 25 February 2025

Abstract

Purpose Gadolinium-neutron capture therapy (Gd-NCT) employs isotopically enriched Gadolinium (Gd) and thermal neutrons to selectively target cancer cells. This study investigated the targeting efficacy of ^{157}Gd-DOTA-PSMA (Prostate-Specific Membrane Antigen) in prostate cancer and explored its potential applications in Gd-NCT.

Methods and results We developed ^{157}Gd-DOTA-PSMA, a novel theranostic bio-gadolinium agent specifically designed for magnetic resonance imaging (MRI)-guided Gd-NCT. ^{68} Ga-DOTA-PSMA positron emission tomography-computed tomography (PET/CT) imaging showed peak radiotracer uptake at 2 h post-injection, with a tumor-to-non-tumor (T/NT) ratio of 6.95 ± 0.60. MRI analysis confirmed a stable T_1 signal enhancement 2 h post-injection. Time-of-flight inductively coupled plasma mass spectrometry (TOF-ICP-MS) revealed significantly elevated Gd concentrations in 22Rv1 tumor compared to PC-3 tumor and other healthy organs. ICP-MS analysis showed Gd concentrations of 165.69 μg [Gd]/g in 22Rv1 tumors and 35.25 μg [Gd]/g in blood, yielding a tumor-to-blood (T/B) ratio of 4.65 ± 0.54 and a T/NT ratio of 3.65 ± 0.49. Neutron irradiation with ^{157}Gd-DOTA-PSMA reduced cell viability, inhibited colony formation, and induced DNA damage and apoptosis in 22Rv1 cells. In 22Rv1 mice, γ-H2AX levels peaked at 6 h post-irradiation, accompanied by an increase in pro-apoptotic proteins and a decrease in anti-apoptotic proteins over 24 h. In the NCT group following the injection of ^{157}Gd-DOTA-PSMA, there was effective suppression of tumor growth without a loss of body weight, resulting in a 1.7-fold increase in median survival compared to control group.

Conclusions ^{157}Gd-DOTA-PSMA, as a theranostic bio-gadolinium agent designed for targeted Gd-NCT in prostate cancer, represents a novel therapeutic approach and broadens the scope of potential applications of neutron capture therapy.

Keywords Neutron capture therapy · PSMA · Prostate cancer · PET/CT · MRI · Molecular imaging

Abbreviations

BNCT	Boron neutron capture therapy
BPA	Boronophenylalanine
BSH	Sodium mercaptoundecahydro-closo-dodecaborate
DMF	N,N-Dimethylformamide
D-D	Deuterium-deuterium
DSBs	Double-strand breaks
EPR	Enhanced permeability and retention
Gd-NCT	Gadolinium-neutron capture therapy
Gd	Gadolinium

✉ Fei Li
lifei007@139.com

✉ Xiaoxi Pang
frankpang@foxmail.com

1 Department of Nuclear Medicine, The Second Affiliated Hospital of Anhui Medical University, Hefei 230601, Anhui, China

2 School of Basic Medical Sciences, Anhui Medical University, Hefei 230032, Anhui, China

3 School of Second Clinical Medical, Anhui Medical University, Hefei 230032, Anhui, China

4 Department of Oncology, The Second Affiliated Hospital of Anhui Medical University, Hefei 230601, Anhui, China

5 Department of Urology, The Second Affiliated Hospital of Anhui Medical University, Hefei 230601, Anhui, China

6 Institute of Plasma Physics, Hefei Institutes of Physical Science, Chinese Academy of Sciences, HefeiAnhui 230031, China

Gd_2O_3	Gadolinium oxide
4He	Alpha
HR-MS	High-resolution mass spectrometry system
HPLC	High performance liquid chromatography
HOBT	1-Hydroxybenzotriazole
ICP-MS	Inductively coupled plasma mass spectrometry
IF	Immunofluorescence
IHC	Immunohistochemical
^{7}Li	Lithium-7
LET	Linear energy transfer
MRI	Magnetic resonance imaging
MALDI	Matrix-assisted laser desorption ionization
NCT	Neutron capture therapy
PET/CT	Positron emission tomography/computed tomography
PSMA	Prostate specific membrane antigen
PTFE	Polytetrafluoroethylene
SPPS	Solid-phase peptide synthesis
T/NT	Tumor-to-non-tumor
TOF-ICP-MS	Time-of-flight inductively coupled plasma mass spectrometry
T/B	Tumor-to-blood
Wb	Western blot

Introduction

Neutron capture therapy (NCT), comprising primarily boron neutron capture therapy (BNCT) and Gd-NCT, has gained significant attention due to its high linear energy transfer (LET) and potential for enhanced cancer treatment efficacy (Capala et al. 2023; Ali 2020). These therapies present an innovative strategy for selectively targeting malignant tumors while potentially minimizing the side effects associated with traditional treatments such as chemotherapy and X-ray radiotherapy (Allen et al. 2017).

BNCT, a sophisticated binary modality of radiotherapy, is progressively being integrated into clinical practice (Malouff et al. 2021). This approach uses thermal and epithermal neutrons, along with Boron-10 enriched compounds, to precisely target tumor cells. Upon thermal neutron irradiation, Boron-10 captures the neutrons, resulting in the production of alpha (^{4}He) particles and lithium-7 (^{7}Li) particles, which are highly effective in eradicating cancer cells (Malouff et al. 2021; Soloway et al. 1998). Conversely, Gd-NCT uses the unique properties of Gd, which has a neutron capture cross-section approximately 66 times greater than that of Boron-10 (Okada et al. 2023; Hosmane et al. 2012; Lai et al. 2023). Following thermal neutron capture, Gd emits high-energy gamma rays (1330 keV), potent enough to induce tumor cell destruction (Shih and Brugger 1992). Furthermore, Gd fulfills a dual role as an MRI contrast agent by shortening T_1 relaxation time, thereby enhancing visualization of tumors near normal tissues during treatment, and facilitating better diagnostic accuracy and real-time monitoring of therapeutic responses (Truillet et al. 2015; Telgmann et al. 2013).

PSMA is a well-established target in prostate cancer, exhibiting increased expression as the disease progresses to metastatic stages (Perner et al. 2007). Radionuclide therapies such as $^{177}Lu/^{225}Ac$-PSMA have been explored for prostate cancer treatment; however, significant side effects, including bone marrow suppression and radiation-induced salivary gland dysfunction, have been observed in clinical trials (Fendler et al. 2017; Kratochwil et al. 2016). $^{177}Lu/^{225}Ac$ is a radioactive isotope that keep emitting radiation in the bloodstream before elminated, potentially harming healthy organs. In contrast, ^{157}Gd-DOTA-PSMA is non-radioactive and only causes localized tumor damage under circumstance that it accumulates in the tumor and is exposed in thermal neutrons. To address these limitations, we developed ^{157}Gd-DOTA-PSMA, a novel theranostic bio-gadolinium agent designed for MRI-guided neutron capture therapy in prostate cancer. This study evaluates the PSMA-targeting efficacy of ^{157}Gd-DOTA-PSMA and investigates its potential applications in Gd-NCT.

Materials and methods

Materials and equipment

The Gd standard solution, with a concentration of 1000 μg/ml, was procured from the Beijing Nonferrous Metals Research Institute, Beijing, China. All additional chemicals, solvents, and reagents were supplied by Sigma-Aldrich, St. Louis, MO, USA. Key equipment and biochemicals used in this study included a Germanium gallium generator from New Radiomedicine Technology Co., Ltd., Chengdu, China, and antibodies such as PSMA, γ-H2AX, Bax, Bcl-2, PCNA, and p53, which were sourced from Abcam and Cell Signaling Technology (USA). Human prostate cancer cell lines, 22Rv1 (RRID: CVCL1045) and PC-3 (RRID: CVCLE2RM), were obtained from Wuhan Pricella Biotechnology Co., Ltd., Wuhan, China. All human cell lines have been authenticated using STR profiling, and it has been confirmed that they were derived from mycoplasma-free cells. Biochemical reagents, including RPMI 1640 medium, phosphate-buffered saline, and fetal bovine serum, were supplied by Shanghai Basalmedia Technologies Co., Ltd., Shanghai, China. Analytical equipment included a 9.4 T animal MRI scanner from United Imaging Healthcare, Shanghai, China, an animal PET/CT

scanner from RAYSOLUTION Healthcare Co., Ltd, Hefei, China, a TOF-ICP-MS system from TOFWERK AG, Thun, Switzerland, an ICP-MS system from Thermo Fisher Scientific, Waltham, USA, a High-Resolution Mass Spectrometry (HR-MS) system and High Performance Liquid Chromatography (HPLC) from SHIMADZU, Kyoto, Japan.

Male SPF-grade nude mice (Six-week-old), were purchased from Ziyuan Experimental Animal Technology Co., Ltd., Hangzhou, China and housed in the Animal Experiment Center of Our University. A thermal-neutron beam was produced at the Institute of Energy, Hefei Comprehensive National Science Center, using a deuterium-deuterium (D-D) neutron generator, which produces 2.5 MeV neutrons at a rate of 2.5×10^8 neutrons per second. The generator operated at an accelerator voltage of 80 kV and a current of 9.3 mA. Neutrons were moderated to thermal neutrons, with a flux of approximately 4.1–4.4 $\times$ 10^8 neutrons/cm^2. After anesthesia, the tumor-bearing mice were fixed on a self-made 3D printed cell irradiation device. This device was designed to expose mouse tumors to neutrons as much as possible to minimize the exposure of surrounding tissues to neutron radiation. Neutron irradiation lasted for about 2–3 h.

All experimental procedures were conducted in accordance with the guidelines of the Institutional Animal Experimentation Ethics Committee of Anhui Medical University under Grant No. LLSC20232209.

Synthesis of ^{157}Gd -DOTA-PSMA and molecular docking

The DOTA-PSMA Peptides were synthesized by Anhui Guoping Pharmaceutical Co., Ltd., Hefei, China, using standard solid-phase peptide synthesis (SPPS) techniques. We designed a DOTA-PSMA ligand in our paper, similar to PSMA-617. We design DOTA-PSMA in the form of direct chain to minimize the intake of salivary glands and other important organs.The synthesis begins with soaking 2-CL resin in a vertical reactor, followed by the coupling of Fmoc-Arg(Pbf)-OH and 1-Hydroxybenzotriazole (HOBT) under nitrogen gas. Fmoc groups are then cleaved using a 20% piperidine/DMF solution. The remaining Fmoc-protected amino acids are sequentially coupled, and DOTA is added to the C-terminus of the peptide chain. The peptide is cleaved from the resin, precipitated with anhydrous ether, and purified by HPLC, achieving a final purity of about 95%, confirming the successful synthesis of DOTA-PSMA.

The synthesis of ^{157}Gd-DOTA-PSMA involved dissolving the DOTA-PSMA peptide in a 30% acetonitrile–water solution, followed by the addition of an excess Gd standard solution(1000ug/ml), The ratio of DOTA-PSMA to Gd solution is 1 mg: 0.3 ml. The pH of the reaction mixture was adjusted to approximately 7 using ammonium bicarbonate, and the solution was stirred overnight. The resulting ^{157}Gd-DOTA-PSMA complex was successfully synthesized and subsequently underwent further purification. Chromatographic separation was achieved using a 20 mm $\times$ 250 mm column packed with Diagsol stationary phase (8 μm particle size), with a gradient elution ranging from 10 to 65% over a period of 45 min.

Molecular docking studies were conducted to investigate covalent interactions between the carboxyl group of DOTA and the amino group of the PSMA protein side chains, resulting in a stable covalent structure. Further molecular docking with Gd-ions was performed, and the binding free energies for both docking interactions were calculated independently to assess the stability and affinity of the synthesized complexes.

Preparation of ^{68}Ga-DOTA-PSMA

A total of 50 μg of DOTA-PSMA peptide was dissolved in 0.5 mol/l sodium acetate buffer to create an appropriate environment for labeling. 0.1 mol/l Hydrochloric acid was utilized to elute the germanium-gallium generator and obtain the ^{68}Ga radionuclide. The labeling reaction was performed at 95 °C in a sodium acetate buffer with a pH range of 3 to 4, and maintained for 15 min to ensure optimal binding between the ^{68}Ga radionuclide and the DOTA.

Monitoring of Biodistribution Dynamics.

Normal mice(n = 15),22Rv1(n = 12) and PC-3(n = 12) xenograft models were administered intravenous (i.v.) injections of ^{68}Ga-DOTA-PSMA (3.7 MBq, 100 μl) via the tail vein, three rats were included at each observation time point. Following the injections, the mice were euthanized through cervical dislocation, and their organs were carefully excised and weighed. The radioactivity of each organ was measured using a γ-counter to calculate the percentage of the injected dose per gram of tissue (%ID/g), providing insights into the distribution of the radiotracer. To gain a more comprehensive understanding of the biodistribution over time, PET/CT imaging was conducted at multiple time points after the administration of ^{68}Ga-DOTA-PSMA. This imaging technique allowed for real-time visualization of the radiotracer's dynamic distribution, facilitating the observation of how its accumulation in both the tumor and surrounding organs changed over time.

Biodistribution analysis of ^{157}Gd-DOTA-PSMA

The biodistribution of ^{157}Gd-DOTA-PSMA was assessed using 9.4 T animal MRI scanner, ICP-TOF–MS imaging, and ICP-MS quantification, guided by dynamic time windows derived from previous nuclear medicine imaging and biodistribution studies. The 9.4 T animal MRI imaging employed

Gd as a T_1 contrast agent to evaluate T_1 enhancement in 22Rv1 tumor-bearing mice (n = 3). MRI Imaging was performed both before and after the administration of ^{157}Gd-DOTA-PSMA (13.4 mg [^{157}Gd] / kg, 100 μl) to visualize changes in gadolinium accumulation in the tumors and various organs.

For ICP-TOF–MS imaging, tissue samples were collected from 22Rv1 xenograft models (n = 3) following the injection of ^{157}Gd-DOTA-PSMA (13.4 mg [^{157}Gd] / kg, 100 μl). The mice were euthanized, and their organs were carefully excised, snap-frozen, and sectioned for further analysis. To visualize the localization of Gd in the harvested tissues, a combination of matrix-assisted laser desorption ionization (MALDI) with laser ablation and ICP-TOF–MS imaging techniques was employed. For Gd quantification via ICP-MS, freeze-dried tissue samples were weighed and placed in cleaned Polytetrafluoroethylene (PTFE) digestion vessels. A mixture of 1 ml of nitric acid, 0.5 ml of hydrochloric acid, and 2 drops of hydrofluoric acid was added to each vessel. The vessels were then sealed and subjected to a microwave digestion program to ensure the complete dissolution of the samples. Following digestion, the resulting solutions were diluted with ultrapure water before being analyzed using ICP-MS for accurate quantification of Gd content.

Biological effects of Gd-NCT in vitro assays

To evaluate the effects of ^{157}Gd-DOTA-PSMA on cell viability and radiosensitivity, we implemented a series of in vitro assays using the CCK-8 methodology and colony formation assays. 22Rv1 Cells were treated with varying concentrations (0–500 μg/ml) of ^{157}Gd-DOTA-PSMA to establish a concentration–response relationship regarding cytotoxic effects. Following treatment, 22Rv1 cells were subjected to thermal neutron irradiation to assess the compound's ability (0–100 μg/ml) to enhance cell death and inhibit growth. During this process, 22Rv1 cells in the experimental group were incubated with 157Gd-DOTA-PSMA for 2 h before undergoing neutron irradiation. Following the incubation period, the cell culture medium was replaced with fresh medium to eliminate any potential influence of extracellular factors on the experimental results. We performed colony formation assays to quantify the long-term effects of combined treatment with ^{157}Gd-DOTA-PSMA and neutron irradiation on 22Rv1 cell proliferation. We established both irradiated and non-irradiated control groups, further dividing them into subgroups based on treatment administration: NCT + Gd + , NCT + Gd − , NCT − Gd − , and NCT − Gd + . To investigate DNA damage resulting from the treatments, γ-H2AX immunofluorescence staining was conducted, enabling the visualization of DNA double-strand breaks in the treated 22Rv1 cells.

Biological effects of Gd -NCT in vivo experiments

The study focused on the therapeutic potential of combining ^{157}Gd-DOTA-PSMA with neutron irradiation in xenograft models. We established both irradiated and non-irradiated control groups and divided them into subgroups based on treatment administration (NCT + Gd + , NCT + Gd − , NCT − Gd − , NCT − Gd +). In the NCT + Gd + group, 22Rv1 xenograft models (n = 3) were administered ^{157}Gd-DOTA-PSMA (13.4 mg [^{157}Gd] / kg, 100 μl) via tail vein injection before undergoing 2 h of targeted thermal neutron irradiation using a 3D-printed acrylic frame.

Subsequent experiments assessed biological markers, including γ-H2AX to quantify DNA double-strand breaks, Bcl-2 and Bax to evaluate the balance between anti-apoptotic and pro-apoptotic signaling, as well as p53 and PCNA as indicators of cell proliferation and growth. These markers were analyzed using Wb analysis to determine their expression levels in treated versus control groups, providing insight into the efficacy of the combined NCT and ^{157}Gd-DOTA-PSMA treatment. Tumor sections were processed and stained using a TUNEL kit, enabling the detection of DNA fragmentation indicative of apoptosis.

Statistical analysis

Data were analyzed using SPSS 23.0 and GraphPad Prism 9.3.0. Results were expressed as mean ± standard deviation $\left(\overline{X} \pm SD\right)$. An independent sample t-test or a paired t-test was employed for data analysis. A significance level of $p < 0.05$ was considered statistically significant.

Results

Synthesis and characterization of ^{157}Gd-DOTA-PSMA

The synthesis of ^{157}Gd-DOTA-PSMA was successfully achieved via SPPS techniques, as illustrated in Fig. 1A. Characterization of the purified DOTA-PSMA peptide was performed using HRMS in positive ion mode (ESI^+), yielding an m/z value of 1016.13, in close agreement with the detected value of 1015.70, as shown in Fig. 1B. HPLC analysis revealed a chemical purity of 94.12% for the DOTA-PSMA peptide, as shown in Fig. 1C. After chelation with Gd, mass spectrometry analysis confirmed the successful incorporation of Gd, as evidenced by the expected mass shift. The HRMS of the gadolinium-chelated (^{157}Gd-DOTA-PSMA) exhibited an m/z value of 1170.00, consistent with the detected value of 1170.39, as shown in Fig. 1D. HPLC analysis of the ^{157}Gd-DOTA-PSMA peptide demonstrated a purity of 95.03%, as shown in Fig. 1E. Molecular docking studies showed that the binding free energy for the covalent

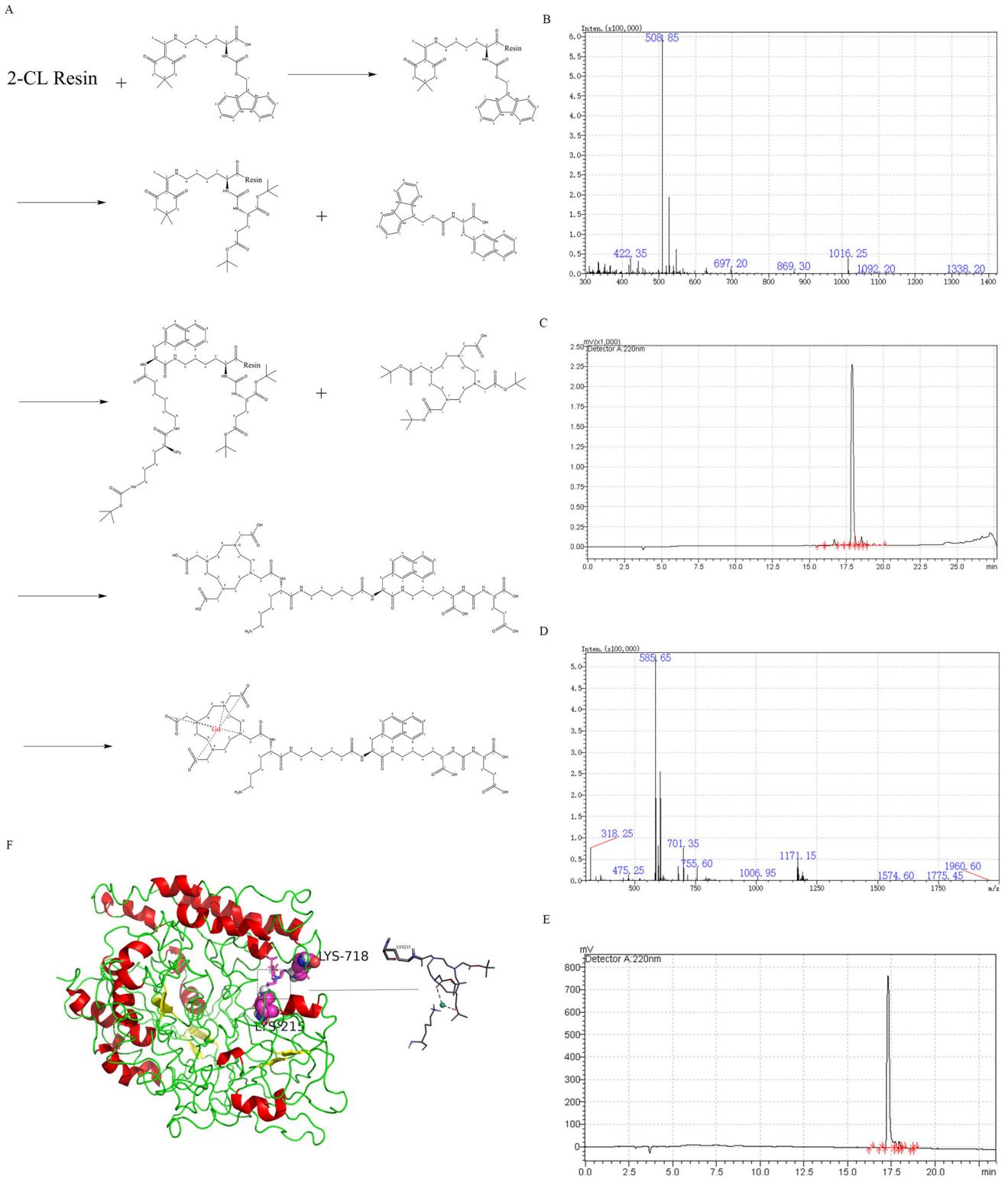

Fig. 1 Synthesis and Characterization of ^{157}Gd-DOTA-PSMA. **A** Successful synthesis via SPPS. **B** HRMS analysis of DOTA-PSMA showed an observed m/z of 1015.70, close to the theoretical value of 1016.13.**C** HPLC analysis indicated a chemical purity of 94.12% for DOTA-PSMA. **D** Gd incorporation was confirmed by mass spectrometry, with HRMS revealing an m/z of 1170.00 compared to the theoretical value of 1170.39. **E** HPLC analysis of ^{157}Gd-DOTA-PSMA demonstrated a purity of 95.03%. **F** Visualization of the molecular docking results, showing the binding interactions between DOTA, PSMA, and Gd ions

docking between DOTA and PSMA was calculated to be -5.39 kcal/mol, while the binding of the DOTA-PSMA complex with Gd ions resulted in a free energy of -4.35 kcal/mol. These non-covalent interactions involved the coordination of Gd ions and the carbonyl oxygen atoms of the DOTA ester group. The results are shown in Fig. 1F.

Identifying PSMA-related targets

This study provides a comprehensive investigation into the targeting specificity of PSMA by evaluating its expression in two human prostate cancer cell lines and corresponding tumor-bearing mouse models. IF analysis revealed strong PSMA-specific fluorescence in 22Rv1 cells (Fig. 2A & E), confirming elevated PSMA expression levels in these cells. Furthermore, Wb analysis of protein lysates from tumor tissues of both mouse models showed significantly higher PSMA expression in 22Rv1 tumors compared to PC-3 cells (Fig. 2B & F), further validating PSMA as a specific target. IHC analysis of tumor sections supported these findings, demonstrating robust PSMA staining in 22Rv1 tumors, while PC-3 tumors exhibited minimal expression, emphasizing the marked difference in PSMA levels between the cell lines (Fig. 2C & G). IF analysis of tumor sections revealed the localization of PSMA at the cell membrane provided, further supporting its potential as a membrane-bound target for therapeutic interventions in prostate cancer (Fig. 2D & H).

^{68}Ga-DOTA-PSMA dynamic biodistribution

Our results indicated that, using ^{68}Ga-DOTA-PSMA micro-PET/CT, 22Rv1 tumor-bearing mice exhibited significantly higher uptake levels and optimal targeting at 2 h (Fig. 3A & Supplementary Table 1). In biodistribution experiments with healthy mice, the ^{68}Ga-DOTA-PSMA probe was cleared through the kidneys via urine, as shown in Fig. 3B. 22Rv1 tumor-bearing mice demonstrated high tumor tissue uptake, peaking at 27.06 ± 2.55%ID/g at 2 h (Fig. 3C & Supplementary Table 2), while PC-3 tumor-bearing mice exhibited significantly lower uptake at 6.23 ± 0.79%ID/g (Fig. 3D). This difference in uptake was statistically significant ($p < 0.01$).

Biodistribution of ^{157}Gd-DOTA-PSMA by MRI and MS

This study used 9.4 T MRI to monitor 22Rv1 tumor-bearing mice following the administration of ^{157}Gd-DOTA-PSMA. The optimal drug distribution was observed at 2 h post-injection, during which substantial T_1 enhancement was evident in the tumors, offering superior resolution of intertumoral details compared to PET/CT imaging, with minimal enhancement seen in non-targeted organs (Fig. 3E). These observations confirm the potential of ^{157}Gd-DOTA-PSMA as a viable neutron capture agent for NCT.

TOF-ICP-MS analysis confirmed that Gd concentrations in 22Rv1 tumors were significantly higher than those in PC-3 tumors and healthy organs (Fig. 3G). These results, supported by MRI data, highlight the strong tumor-targeting capability of ^{157}Gd-DOTA-PSMA as a Gd-NCT agent. Furthermore, Gd quantification via ICP-MS revealed an average Gd concentration of 165.69 μg [Gd]/g in 22Rv1 tumors and 35.25 μg [Gd]/g in blood, resulting in a T/B ratio of 4.65 ± 0.54 and a T/NT ratio of 3.65 ± 0.49 (Fig. 3F). Gd retention in the tumors exceeded the injected dose by more than ten-fold, with approximately 19.09% of the compound localized in the tumor tissue, closely reflecting the biodistribution of ^{68}Ga-DOTA-PSMA in 22Rv1 tumors.

Radiobiological effects of Gd-NCT in vitro assays

The results indicated that, without exposure to neutron irradiation, cell viability remained stable across various concentrations of ^{157}Gd-DOTA-PSMA. At a therapeutic concentration of 100 μg/ml, no observable cytotoxic effects were detected. However, at an elevated concentration of 500 μg/ml, a marked decrease in cell viability, demonstrating a dose-dependent cytotoxic effect at higher concentrations. Overall, ^{157}Gd-DOTA-PSMA exhibits low cytotoxicity within the therapeutic dosage range (Fig. 4A).

Following exposure to thermal neutron irradiation, 22Rv1 cells treated with 50 μg/ml of ^{157}Gd-DOTA-PSMA showed moderate suppression of cell viability ($p < 0.05$). In the 100 μg/ml group, cell viability decreased markedly after irradiation, with significant differences compared to the control group ($p < 0.001$) (Fig. 4B). These findings suggested that ^{157}Gd-DOTA-PSMA enhances the inhibitory effects of thermal neutron irradiation, supporting its potential utility in radiobiology applications.

After thermal neutron irradiation, 22Rv1 cells showed a significant reduction in colony formation compared to the control groups, indicating that ^{157}Gd-DOTA-PSMA enhances the effects of neutron irradiation, leading to a reduction in cell proliferation and survival (Fig. 4C & D). Moreover, γ-H2AX IF staining showed strong fluorescence in cells treated with Gd-NCT, indicating significant DNA double-strand breaks (Fig. 4E). This increased fluorescence is a marker of DNA damage, suggesting that the Gd-NCT effectively induces DNA damage, which is critical for sensitizing cancer cells to radiation therapy.

Radiobiological effects of Gd-NCT in vivo experiments

In the study, we initially identified the optimal time window for observing the effects of NCT. The results revealed

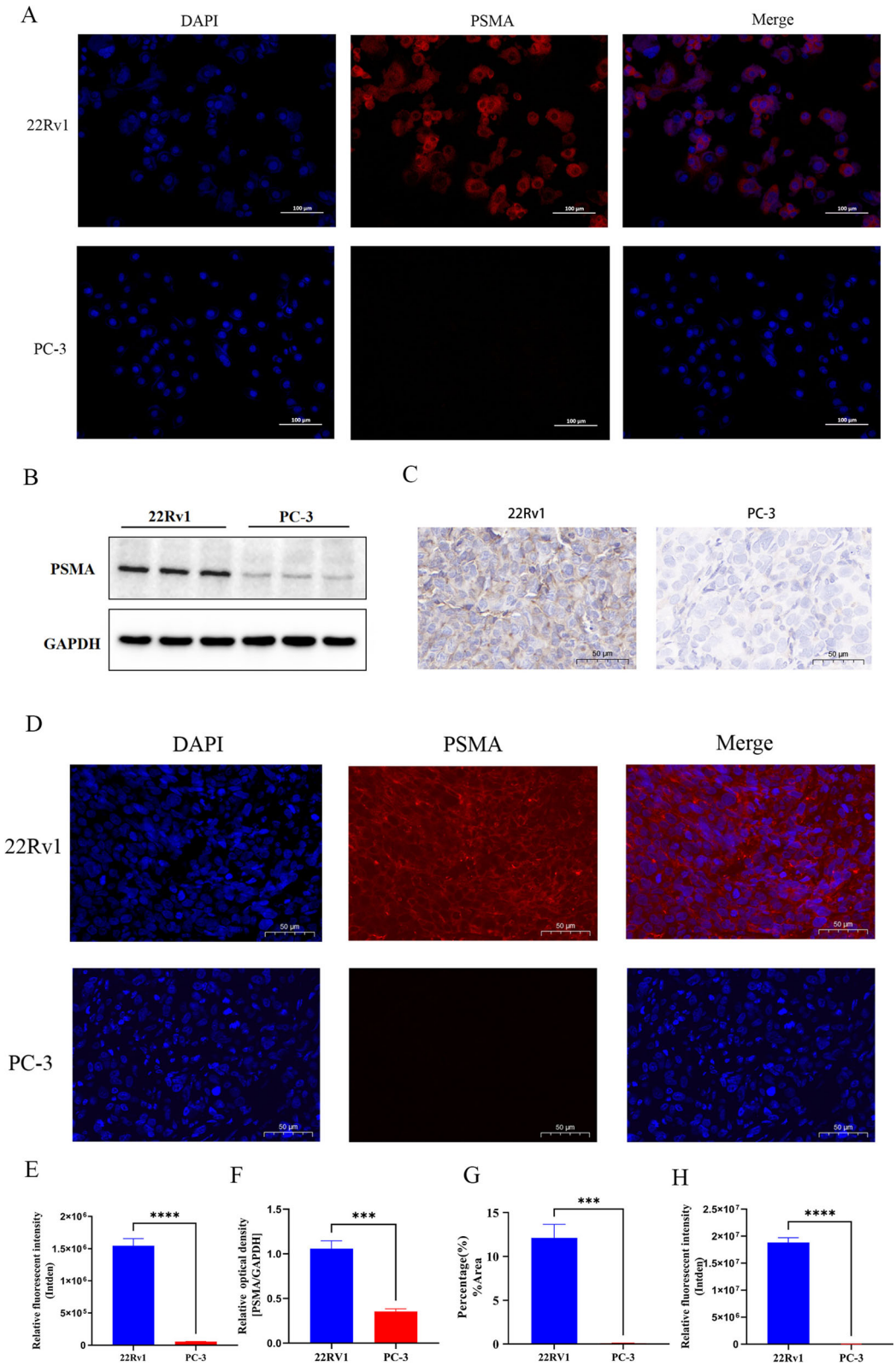

Fig. 2 Identification of PSMA-Related Targets. **A** IF analysis demonstrates high PSMA expression (red) in 22Rv1 cells compared to PC-3 cells, with nuclei stained using DAPI (blue). Scale bar: 100 μm. **B** Wb analysis reveals a prominent PSMA band (60–65 kD) in 22Rv1 cells, while a weaker band is observed in PC-3 cells. **C** IHC shows strong PSMA expression in 22Rv1 xenografts, with lower expression noted in PC-3 tumors. Scale bar: 50 μm. **D** IF analysis reveals increased PSMA levels in 22Rv1 xenografts (red), with nuclei stained in blue. Scale bar: 50 μm. E–H) Data analyses: Cell IF Data Analysis (**E**); Wb data analysis (**F**); IHC data analysis (**G**); Tissue IF data analysis (**H**)

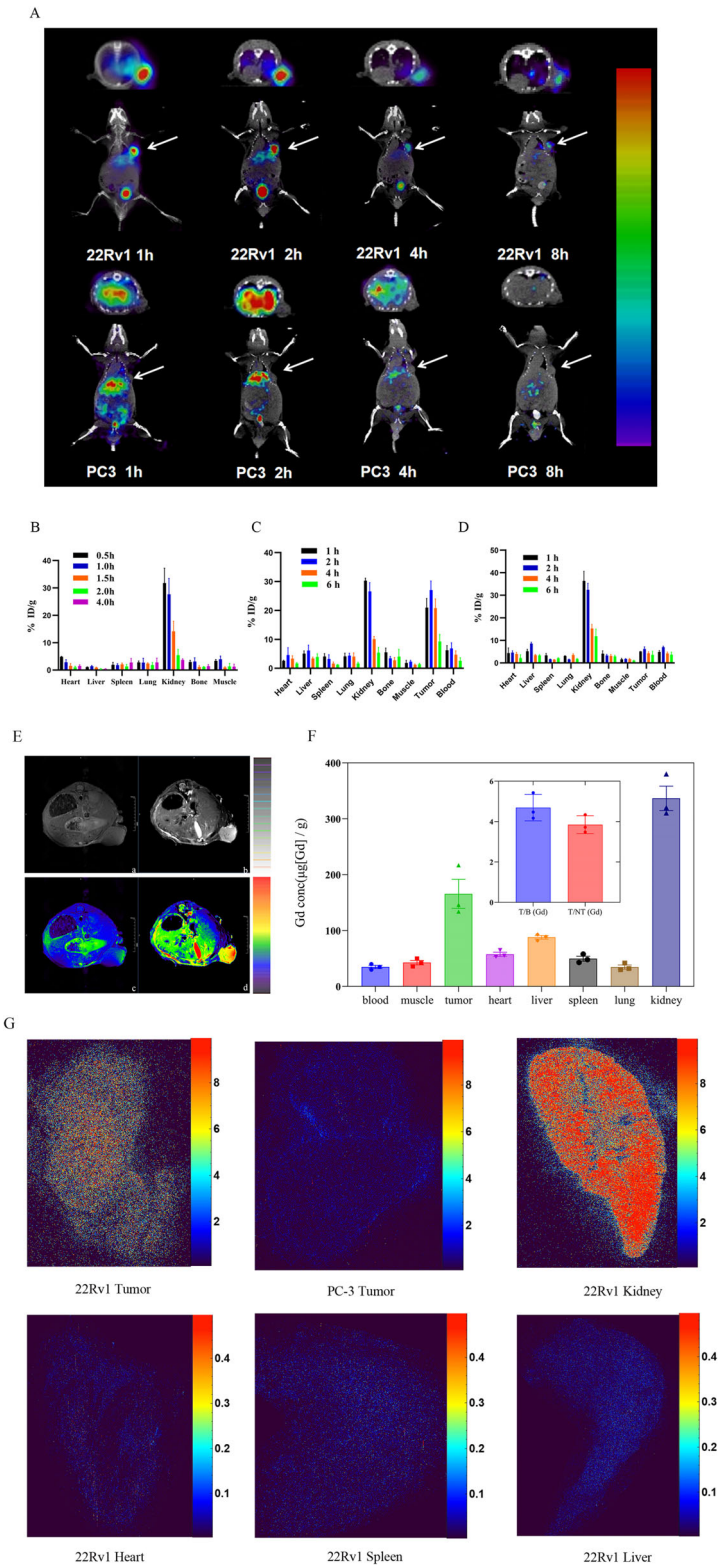

Fig. 3 Dynamics of ^{68}Ga-DOTA-PSMA and ^{157}Gd-DOTA-PSMA Biodistribution. **A** PET/CT imaging of 22Rv1 and PC-3 xenografts at multiple time points. **B** Biodistribution of ^{68}Ga-DOTA-PSMA in healthy mice over various time intervals post-injection. **C** Biodistribution of ^{68}Ga-DOTA-PSMA in 22Rv1 tumor-bearing mice at different post-injection times. **D** Biodistribution of ^{68}Ga-DOTA-PSMA in PC-3 tumor-bearing mice at various post-injection times. **E** T_1-weighted MRI scans of 22Rv1 tumor-bearing mice before and after ^{157}Gd-DOTA-PSMA injection. **F** Quantification of Gd levels in tissues using ICP-MS. **G** Analysis of tissue cryosections using TOF-ICP-MS for Gd localization after injection of ^{157}Gd-DOTA-PSMA

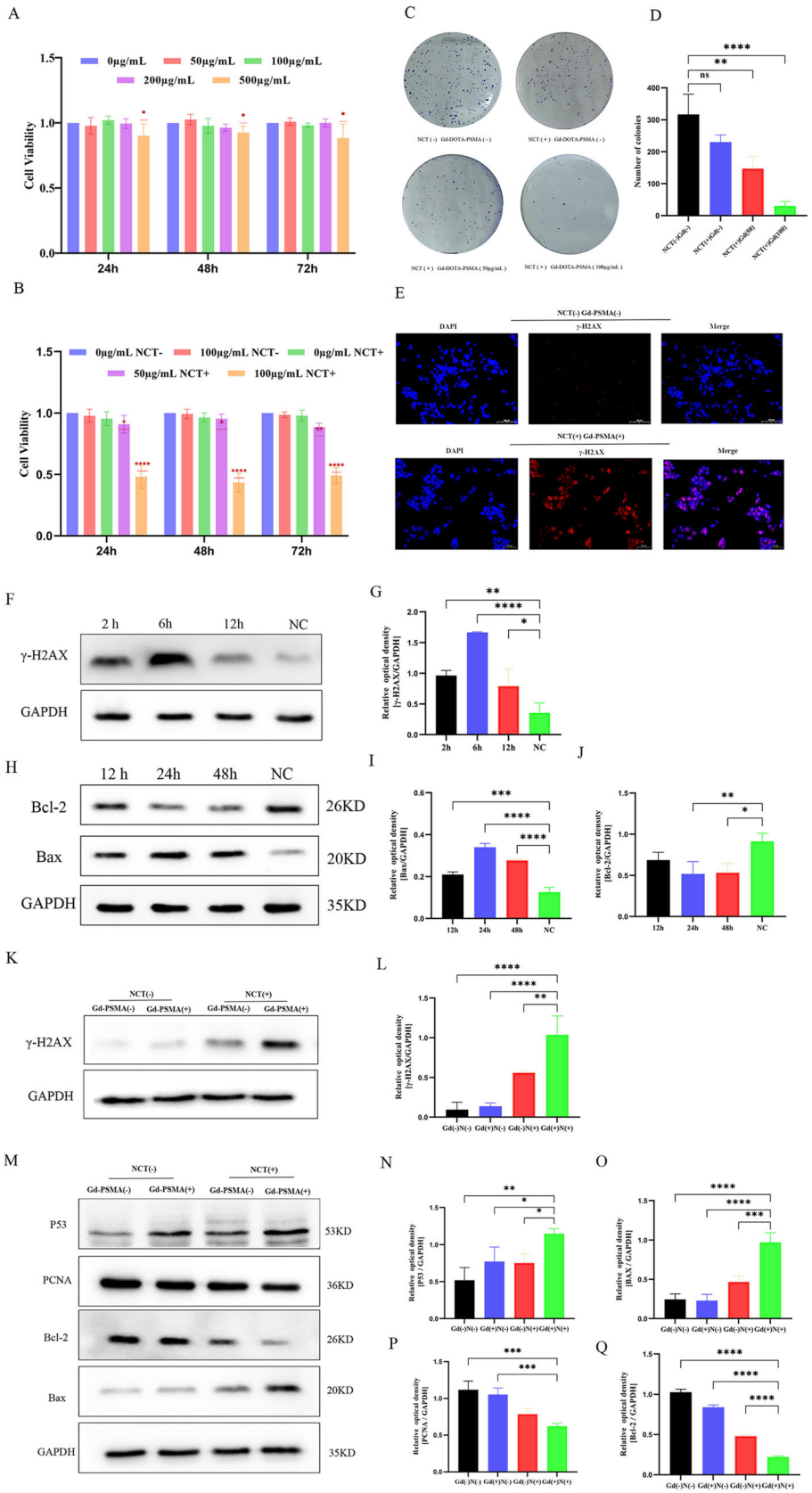

Fig. 4 Radiobiological Effects of Gd-NCT In Vitro and In Vivo Assays. **A** The cck-8 assay demonstrates stable cell viability across various concentrations of ^{157}Gd-DOTA-PSMA, with no toxicity observed at 100 μg/ml (therapeutic dose) and moderate suppression at 500 μg/ml (*: $p < 0.05$). **B** Following thermal neutron irradiation, the 50 μg/ml group showed moderate suppression, while the 100 μg/ml group experienced significant reduction in cell viability, indicating enhanced inhibitory effects. **C** The colony formation indicates a significant decrease in colony count for 22Rv1 cells treated with ^{157}Gd-DOTA-PSMA after neutron irradiation in comparison to control groups. **D** Quantitative evaluation of the effect of Gd-NCT on colony formation: Gd-DOTA-PSMA-targeted NCT can significantly inhibit the formation of cell colonies. **E** γ-H2AX IF staining shows intense fluorescence in cells treated with ^{157}Gd-DOTA-PSMA after neutron irradiation, signifying extensive DNA double-strand breaks. **F** γ-H2AX expression peaks about six hours post-neutron irradiation. **G** γ-H2AX expression significantly increases at six hours. **H** Bax expression peaks, while Bcl-2 expression reaches its lowest point at approximately 24 h post-irradiation. **I** Bax expression significantly increases at 24 h. **J** Bcl-2 expression significantly decreases at 24 h. **K** γ-H2AX expression is significantly upregulated in the Gd-NCT group (NCT + Gd +) compared to other groups. **L** γ-H2AX expression shows a significant increase in the Gd-NCT group. **M** p53 (**N**) and Bax (**O**) expression significantly upregulated in the Gd-NCT group; PCNA (**P**) and Bcl-2 (**Q**) expression significantly decrease in the Gd-NCT group

that γ-H2AX expression peaked at approximately 6 h post-irradiation (Figs. 4F & G). Moreover, 24 h post-treatment, the levels of the pro-apoptotic protein Bax peaked, while the expression of the anti-apoptotic protein Bcl-2 levels was significantly reduced (Figs. 4H-J).

Subsequent experiments were conducted at this optimal time point to evaluate DNA damage, apoptosis, and cell proliferation in tumor-bearing mice. The findings indicated that in 22Rv1 tumor-bearing mice treated with Gd-NCT, there was a significant upregulation of γ-H2AX (Figs. 4K & L), the tumor suppressor protein p53 (Figs. 4M &N), and the pro-apoptotic protein Bax (Fig. 4O). Meanwhile, the expression of the proliferation marker PCNA (Fig. 4P) and the anti-apoptotic protein Bcl-2 (Fig. 4Q) was significantly reduced, indicating effective inhibition of tumor growth and promotion of apoptosis in the treated group.

Histological evaluation of normal organs and tumor tissues in 22Rv1 tumor-bearing mice further supported these findings. Tumor tissues in the group receiving Gd-NCT displayed pronounced signs of fragmentation and cellular destruction, whereas histological assessments of major organs such as the heart, liver, spleen, lungs, and kidneys showed no abnormalities (Figs. 5A & B). In the Gd-NCT treatment group, TUNEL showed strong fluorescent signals in the tumor tissues. Compared to the control group, the fluorescent intensity in the treatment group was significantly higher, with a greater proportion of apoptotic cells ($p < 0.001$), indicating that Gd-NCT treatment significantly promoted apoptosis in tumor cells. (Figs. 5C & E). IHC analysis for γ-H2AX showed strong positive staining in the tumor tissues of the Gd-NCT treatment group. Quantitative analysis revealed a significant increase in γ-H2AX expression levels in the Gd-NCT treatment group compared to the control group ($p < 0.0001$) (Fig. 5D & F), indicating an enhanced DNA damage response in tumors subjected to Gd-NCT.

The anti-tumor experiment is schematically illustrated in Fig. 5G-I**.** The study included four groups ($n = 10$ each): (NCT − Gd −), (NCT + Gd −), (NCT + Gd +), (NCT + BPA +) group. The doses of ^{157}Gd-DOTA-PSMA (13.4 mg [^{157}Gd] / kg), BPA (0.85 mg [^{10}B] / kg) which is equivalent to molar amounts. BPA is the only ^{10}B contained delivery admitted for boron neutron capture therapy in clinic. While most tumors can absorb BPA to achieve a therapeutic effect, prostate cancer also takes up BPA; however, it lacks specific targeting for prostate cancer, result in a quite low dose accumulated in tumor. As shown in Fig. 5G**,** the body weights of mice for (NCT + Gd +) treatment groups did not show significant changes over the 33 days during the therapeutic treatments, significantly higher than that in control group. In contrast, the control group exhibited notable weight loss, highlighting the beneficial effects of Gd-NCT on mouse health during the therapeutic regimen. The tumor volume plots shown in Fig. 5H demonstrate that the (NCT + Gd +)-treated mice had the smallest average tumor size among all control group, correlating with the anti-tumor effects of Gd-NCT and suggesting its potential as a promising therapeutic strategy. As shown in Fig. 5I, tumor-bearing mice in (NCT − Gd −) group died within 35 days, The survival rate of tumor bearing mice in (NCT + Gd +) group (61 days) was significantly higher than that in control group, which may be related to the ^{157}Gd-DOTA-PSMA delivering agent. These results indicate that the incorporation of ^{157}Gd-DOTA-PSMA and NCT significantly improves survival and tumor control, potentially paving the way for more effective cancer treatments.

Discussion

This study confirms the feasibility of employing molecular imaging techniques, including PET/CT and MRI, to guide PSMA-targeted Gd-NCT in the treatment of prostate cancer. We investigate the therapeutic efficacy of ^{157}Gd-DOTA-PSMA, emphasizing the importance of dynamic monitoring of drug delivery to optimize treatment outcomes (Monti Hughes and Hu 2023; Jung et al. 2018). The integration of PET/CT, MRI and MS is essential for accurately assessing the biological distribution and concentration of the drug, ultimately improving therapeutic efficacy (Rashid et al. 2016; Stasio et al. 2005). Previous research suggests that real-time MRI monitoring of cancer progression, both before and after Gd-NCT treatment, offers a more accurate evaluation of therapeutic effectiveness (Lai et al. 2023; Ho et al. 2022).

The therapeutic efficacy of ^{157}Gd-DOTA-PSMA relies on delivering a sufficient dose to the tumor while minimizing exposure to healthy tissues, thereby reducing the risk of toxicity associated with neutron irradiation. Achieving this goal necessitates the consideration of three key factors: determining the optimal gadolinium enrichment time window, assessing T/NT and T/B ratios, and ensuring sufficient neutron flux during irradiation (Ho et al. 2022, 2018). In our investigation, we validated the chelation efficacy of the gadolinium compound through HPLC and MS. Molecular docking calculations were also employed to assess the binding energy of relevant compounds, confirming that Gd was present in a chelated form.

Current advancements in boron-based drugs predominantly utilize Boronophenylalanine (BPA) and Sodium borocaptat (BSH) (Barth et al. 2024, 2018). In BNCT, achieving a Boron-10 concentration ratio greater than 3:1 in both T/N and T/B is critical (Okada et al. 2023; Barth et al. 2018; Wang et al. 2022). However, these compounds often exhibit similar accumulation patterns in tumors, normal tissues, and blood, reflecting their non-selective properties, which necessitates continuous intravenous administration (Wang et al. 2022; He et al. 2021). Specifically, BPA demonstrates limited

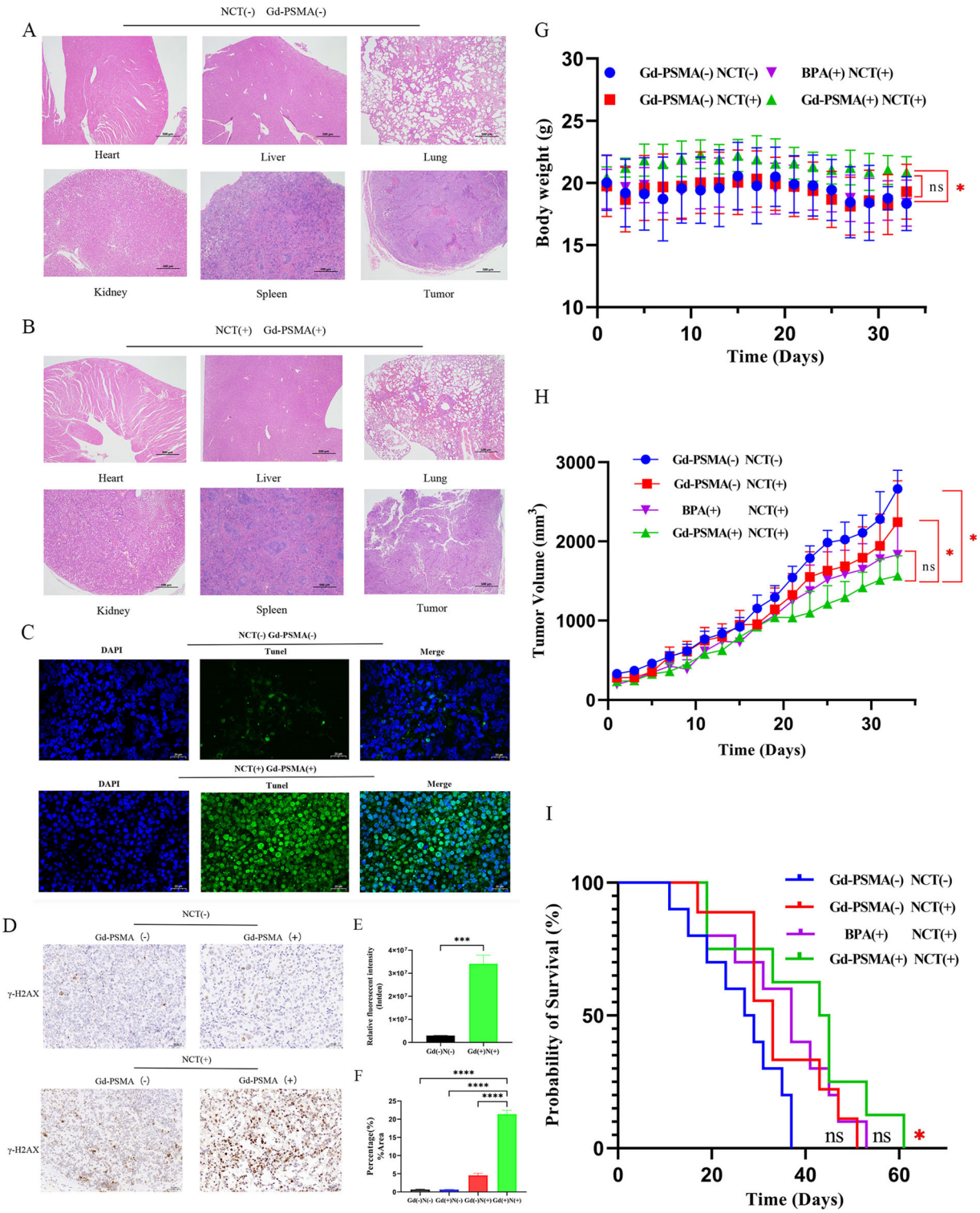

Fig. 5 Radiobiological effects of Gd-NCT on tumor tissue. **A** The organs in the control group (NCT − Gd −) appeared histologically normal. **B** Tumor tissues from the Gd-NCT group displayed considerable fragmentation and damage, indicating a robust therapeutic response. **C** TUNEL assay showing strong fluorescent signals in Gd-NCT group tumor tissues. **D** IHC analysis for γ-H2AX showed strong positive staining in the Gd-NCT group. **E**) Data analyses: TUNEL data analysis. F) Data analyses: γ-H2AX IHC data analysis. **G**-**I** Anti-tumor effect of Gd-NCT in Vivo in 22 Rv1 tumor-bearing mice with various treatments. **G** Body weights of tumor models with various treatments. **H** Tumor-growth curves of tumor models with various treatments. **I** Kaplan–Meier survival curves of tumor models with various treatments (ns: no statistical difference with the Gd (-) NCT (-). *:$p < 0.05$ with Gd(-) NCT(-)

tumor retention and requires high dosages, up to 350 mg/kg (Monti Hughes and Hu 2023; Zhang et al. 2023; Barth 2009). This underscores the challenges associated with precise tumor targeting and emphasizes the need for improved delivery systems to enhance treatment efficacy. Furthermore, the poor water solubility of BPA and its limited selectivity restrict its capacity for effective tumor targeting. While BSH is more water-soluble, it lacks active targeting mechanisms, reducing its therapeutic effectiveness (Lamba et al. 2021; Kondo et al. 2022; Järvinen et al. 2023). In contrast, Gd-based agents possess a larger reaction cross-section than Boron-10-based agents, allowing for more effective tumor cell destruction through γ-radiation, which is capable of inhibiting tumor growth and proliferation, as demonstrated in this and previous studies (Lai et al. 2023; Ho et al. 2022). Nevertheless, traditional Gd-based agents continue to encounter challenges, including suboptimal targeting and insufficient in vivo stability, which impede their therapeutic potential (Ho et al. 2022, 2018). For instance, in glioblastoma patients, only 6.1% of cancer cell nuclei were found to contain ^{157}Gd-DTPA, indicating inadequate targeting and rapid renal clearance (Ho et al. 2022).

To overcome these limitations, researchers are investigating various delivery systems, including liposomes (Le and Cui 2006a, 2006b), nanomaterials (Ho et al. 2022), and chitosan (Horiguchi et al. 2011). For instance, Lee et al. (Lee et al. 2021) demonstrated that administering ^{157}Gd-DO3A-butanol to CT26 tumor-bearing mice resulted in a 43% reduction in tumor volume compared to controls after 23 days of neutron irradiation. Similarly, studies by Tokumitsu et al. (Tokumitsu et al. 1999) and Kobayashi et al. (Kobayashi et al. 2001) found that ^{157}Gd-nanoCPs accumulated more effectively in tumors exhibited prolonged retention compared to ^{157}Gd-DTPA, leading to superior tumor growth inhibition. Further innovations include gadolinium oxide (Gd_2O_3) as reported by Ho SL et al. (Ho et al. 2018) and Gd@C_{82} nanomaterial by Lee W et al. (Lee et al. 2021), both of which enhance gadolinium delivery and offer potential multifunctional therapeutic benefits. These systems utilize the enhanced permeability and retention (EPR) effect to improve the distribution and accumulation of Gd in tumors (Horiguchi et al. 2011). The effectiveness of these carriers may vary based on tumor type and size, as larger particles can cause embolism, impaired circulation, and increased risk of inflammation or allergic reactions. Gadolinium-based nanomaterials are primarily limited to intraperitoneal or intratumoral injections.

PSMA is highly expressed in prostate cancer cells, making it an ideal target for both diagnosis and treatment. Previous radionuclide therapies, such as ^{177}Lu- and ^{225}Ac-PSMA, have demonstrated therapeutic efficacy; however, they are also associated with significant side effects, including bone marrow suppression and salivary gland toxicity (Fendler et al. 2017; Kratochwil et al. 2016). As a promising agent in neutron capture therapy, ^{10}B-psma has undergone extensive investigation (Meher et al. 2021). However, its current tumor uptake (4–7 μg/g) falls short of the optimal therapeutic dose of 20–50 μg/g, posing challenges for enhancing ^{10}B-PSMA accumulation (Barth et al. 2018; Wang et al. 2019). Our study shows that ^{68}Ga-DOTA-PSMA PET/CT imaging exhibits peak radiotracer uptake 2–3 h post-injection, with a high T/NT ratio of 6.95 ± 0.60. This high specificity and robust tumor accumulation of ^{157}Gd-DOTA-PSMA are crucial for effective neutron capture therapy. ICP-MS confirmed gadolinium concentrations of 165.69 μg [Gd]/g in 22Rv1 tumors versus 35.25 μg [Gd] / g in blood, yielding a T/B ratio of 4.65 ± 0.54 and a T/NT ratio of 3.65 ± 0.49.

DNA damage is considered the most significant cause of mitotic death. Neutron irradiation with ^{157}Gd-DOTA-PSMA significantly reduces cell viability and increases apoptosis by inducing extensive DNA damage, consistent with previous research findings (Ho et al. 2022; Lomax et al. 2013). Complex DNA damage, such as double-strand breaks resulting from high linear energy transfer ionizing radiation during NCT, is challenging to repair (Lomax et al. 2013), contributing to a reduced risk of tumor recurrence. Studies have shown that Gd-NCT generates numerous high-energy particles that inflict direct DNA damage in cancer cells, or indirectly cause damage through the production of reactive OH^- radicals or OH^- ions via interactions with water molecules, leading to further DNA damage (Ho et al. 2022). Additionally, several proteins, including p38, PCNA, Bcl-2, and Bax play roles in both repairing DNA damage and in the process of programmed cell death, or apoptosis (Kondo 2022; Gu et al. 2023; Youle and Strasser 2008). Our study shows that Gd-NCT treatment results in increased expression of the γ-H2AX, the tumor suppressor protein p53, and the pro-apoptotic protein Bax. Simultaneously, it decreases the levels of the cell proliferation marker PCNA and the anti-apoptotic protein Bcl-2. These changes suggest that Gd-NCT boosts DNA damage response and apoptosis while reducing cell survival and proliferation, highlighting its potential as a cancer therapy. This therapeutic effect is primarily due to the ability of Gd to emit γ-rays and internal conversion electrons upon neutron capture, which cause significant DNA damage and changes in the tumor microenvironment (Shamsabadi and Baghani 2024).

Our study has some limitations. Although prostate cancer exhibits high gadolinium uptake, PSMA primarily targets the cell membrane, and optimal effects require the drug to reach the cell nucleus to induce DNA damage and alter the tumor microenvironment. Future research should focus on enhancing the ability of PSMA-targeted drugs to penetrate cells and reach the nucleus. Additionally, normal cells may be damaged following Gd-NCT treatment. We have filed a patent for the protection of healthy tissue. Future research should focus

on determining the optimal dose of ^{157}Gd-DOTA-PSMA, the appropriate neutron flux, and conducting clinical trials for Gd-NCT.

In summary, ^{157}Gd-DOTA-PSMA represents a novel theranostic bio-gadolinium agent with significant potential for targeted neutron capture therapy, expanding the scope of prostate cancer treatment and NCT applications.

Supplementary Information The online version contains supplementary material available at https://doi.org/10.1007/s00432-025-06136-7.

Acknowledgements The authors would like to express their gratitude to EditSprings (https://www.editsprings.cn) for the expert linguistic services provided.

Author contributions L.X.: Data curation, Formal analysis, Investigation, Methodology, Writing – original draft. J.Q.: Investigation, Methodology. C.S.:Formal analysis, Methodology. J.Y.: Investigation, Methodology. R.W.: Data curation, Software. H.C.: Resources Software. Y.D.: Formal analysis, Methodology N. W.: Resources, Validation. L.C.: Resources, Software. B. H.: Conceptualization, Methodology, Validation. N.C.: Methodology, Supervision. P. L.: Resources, Supervision, Validation. F. L.: Resources, Supervision, Validation. X.P.: Conceptualization, Funding acquisition, Supervision, Visualization, Writing–review & editing.

Funding This work was supported by University Natural Science Research Project of Anhui Province [2023AH040380, KJ2021ZD0031]; and Clinical Research Cultivation Program of The Second Affiliated Hospital of Anhui Medical University [2021LCYB08, 2020LCD14].

Data availability No datasets were generated or analysed during the current study.

Declarations

Conflict of interest The authors declare no competing interests.

Ethical approval All experimental procedures were conducted in accordance with the guidelines of the Institutional Animal Experimentation Ethics Committee of Anhui Medical University under Grant No. LLSC20232209.

References

Ali F, Hosmane SN, Zhu Y (2020) Boron chemistry for medical applications. Molecules. https://doi.org/10.1016/j.addr.2017.01.004

Allen C, Her S, Jaffray DA (2017) Radiotherapy for cancer: present and future. Adv Drug Deliv Rev 109:1–2

Barth RF (2009) Boron neutron capture therapy at the crossroads: challenges and opportunities. Appl Radiat Isot 67:S3–S6

Barth RF, Mi P, Yang W (2018) Boron delivery agents for neutron capture therapy of cancer. Cancer Commun (Lond) 38:35

Barth RF, Gupta N, Kawabata S (2024) Evaluation of sodium borocaptate (BSH) and boronophenylalanine (BPA) as boron delivery agents for neutron capture therapy (NCT) of cancer: an update and a guide for the future clinical evaluation of new boron delivery agents for NCT. Cancer Commun (Lond) 44:893–909

Capala J, Hong JA, Vikram B, Coleman CN (2023) Neutron capture therapy: the promise of novel agents and medical facility-based neutron sources. Cancer Biother Radiopharm 38:141–142

De Stasio G, Rajesh D, Casalbore P, Daniels MJ, Erhardt RJ, Frazer BH, Wiese LM, Richter KL, Sonderegger BR, Gilbert B, Schaub S, Cannara RJ, Crawford JF, Gilles MK, Tyliszczak T, Fowler JF, Larocca LM, Howard SP, Mercanti D, Mehta MP, Pallini R (2005) Are gadolinium contrast agents suitable for gadolinium neutron capture therapy? Neurol Res 27:387–398

Fendler WP, Rahbar K, Herrmann K, Kratochwil C, Eiber M (2017) 177Lu-PSMA radioligand therapy for prostate cancer. J Nucl Med 58:1196–1200

Gu L, Li M, Li CM, Haratipour P, Lingeman R, Jossart J, Gutova M, Flores L, Hyde C, Kenjić N, Li H, Chung V, Li H, Lomenick B, Von Hoff DD, Synold TW, Aboody KS, Liu Y, Horne D, Hickey RJ, Perry JJP, Malkas LH (2023) Small molecule targeting of transcription-replication conflict for selective chemotherapy. Cell Chem Biol 30:1235-1247.e6

He H, Li J, Jiang P, Tian S, Wang H, Fan R, Liu J, Yang Y, Liu Z, Wang J (2021) The basis and advances in clinical application of boron neutron capture therapy. Radiat Oncol 16:216

Ho SL, Cha H, Oh IT, Jung KH, Kim MH, Lee YJ, Miao X, Tegafaw T, Ahmad MY, Chae KS, Chang Y, Lee GH (2018) Magnetic resonance imaging, gadolinium neutron capture therapy, and tumor cell detection using ultrasmall Gd2O3 nanoparticles coated with polyacrylic acid-rhodamine B as a multifunctional tumor theragnostic agent. RSC Adv 8:12653–12665

Ho SL, Yue H, Tegafaw T, Ahmad MY, Liu S, Nam SW, Chang Y, Lee GH (2022) Gadolinium neutron capture therapy (GdNCT) agents from molecular to nano: current status and perspectives. ACS Omega 7:2533–2553

Horiguchi Y, Kudo S, Nagasaki Y (2011) Gd@C82 metallofullerenes for neutron capture therapy-fullerene solubilization by poly (ethylene glycol)-block-poly (2-(N, N-diethylamino)ethyl methacrylate) and resultant efficacy in vitro. Sci Technol Adv Mater 12:044607

Hosmane NS, Maguire JA, Zhu Y, Takagaki M (2012) Boron and gadolinium neutron capture therapy for cancer treatment. World Scient. https://doi.org/10.1142/8056

Järvinen J, Pulkkinen H, Rautio J, Timonen JM (2023) Amino acid-based boron carriers in boron neutron capture therapy (BNCT). Pharmaceutics 15:2663

Jung KH, Park JA, Kim JY, Kim MH, Oh S, Kim HK, Choi EJ, Kim HJ, Do SH, Lee KC, Kim KM, Lee YJ, Chang Y (2018) Image-guided neutron capture therapy using the gd-do3a-bta complex as a new combinatorial treatment approach. Contrast Media Mol Imag 2018:3727109

Kobayashi H, Kawamoto S, Saga T, Sato N, Ishimori T, Konishi J, Ono K, Togashi K, Brechbiel MW (2001) Avidin-dendrimer-(1B4M-Gd)(254): a tumor-targeting therapeutic agent for gadolinium

neutron capture therapy of intraperitoneal disseminated tumor which can be monitored by MRI. Bioconjug Chem 12:587–593
Kondo N (2022) DNA damage and biological responses induced by boron neutron capture therapy (BNCT). Enzymes 51:65–78
Kondo N, Hirano F, Temma T (2022) Evaluation of 3-borono-l-phenylalanine as a water-soluble boron neutron capture therapy agent. Pharmaceutics 14:1106
Kratochwil C, Bruchertseifer F, Giesel FL, Weis M, Verburg FA, Mottaghy F, Kopka K, Apostolidis C, Haberkorn U (2016) Morgenstern A 225Ac-PSMA-617 for PSMA-targeted α-radiation therapy of metastatic castration-resistant prostate cancer. J Nucl Med 57:1941–1944
Lai YH, Su CY, Cheng HW, Chu CY, Jeng LB, Chiang CS, Shyu WC, Chen SY (2023) Stem cell-nanomedicine system as a theranostic bio-gadolinium agent for targeted neutron capture cancer therapy. Nat Commun 14:285
Lamba M, Goswami A, Bandyopadhyay A (2021) A periodic development of BPA and BSH based derivatives in boron neutron capture therapy (BNCT). Chem Commun (Camb). https://doi.org/10.1039/D0CC06557A
Le UM, Cui Z (2006a) Biodistribution and tumor-accumulation of gadolinium (Gd) encapsulated in long-circulating liposomes in tumor-bearing mice for potential neutron capture therapy. Int J Pharm 320:96–103
Le UM, Cui Z (2006b) Long-circulating gadolinium-encapsulated liposomes for potential application in tumor neutron capture therapy. Int J Pharm 312:105–112
Lee W, Jung KH, Park JA, Kim JY, Lee YJ, Chang Y, Yoo J (2021) In vivo evaluation of PEGylated-liposome encapsulating gadolinium complexes for gadolinium neutron capture therapy. Biochem Biophys Res Commun 56:823–829
Lomax ME, Folkes LK, O'Neill P (2013) Biological consequences of radiation-induced DNA damage: relevance to radiotherapy. Clin Oncol (r Coll Radiol) 25:578–585
Malouff TD, Seneviratne DS, Ebner DK, Stross WC, Waddle MR, Trifiletti DM, Krishnan S (2021) Boron neutron capture therapy: a review of clinical applications. Front Oncol 11:601820
Meher N, Seo K, Wang S, Bidkar AP, Fogarty M, Dhrona S, Huang X, Tang R, Blaha C, Evans MJ, Raleigh DR, Jun YW, VanBrocklin HF, Desai TA, Wilson DM, Ozawa T, Flavell RR (2021) Synthesis and preliminary biological assessment of carborane-loaded theranostic nanoparticles to target prostate-specific membrane antigen. ACS Appl Mater Interfac 13:54739–54752
Monti Hughes A, Hu N (2023) Optimizing boron neutron capture therapy (BNCT) to treat cancer: an updated review on the latest developments on boron compounds and strategies. Cancers (Basel) 15:4091
Okada S, Nishimura K, Ainaya Q, Shiraishi K, Anufriev SA, Sivaev IB, Sakurai Y, Suzuki M, Yokoyama M, Nakamura H (2023) Development of a gadolinium-boron-conjugated albumin for MRI-guided neutron capture therapy. Mol Pharm 20:6311–6318
Perner S, Hofer MD, Kim R, Shah RB, Li H, Möller P, Hautmann RE, Gschwend JE, Kuefer R, Rubin MA (2007) Prostate-specific membrane antigen expression as a predictor of prostate cancer progression. Hum Pathol 38:696–701
Rashid HU, Martines MAU, Jorge J, de Moraes PM, Umar MN, Khan K, Rehman HU (2016) Cyclen-based Gd3+ complexes as MRI contrast agents: relaxivity enhancement and ligand design. Bioorg Med Chem 245:663–5684
Shamsabadi R, Baghani HR (2024) Impact of gadolinium concentration and cell oxygen levels on radiobiological characteristics of gadolinium neutron capture therapy technique in brain tumor treatment. Radiol Phys Technol 17:135–142
Shih JL, Brugger RM (1992) Gadolinium as a neutron capture therapy agent. Med Phys 19:733–744
Soloway AH, Tjarks W, Barnum BA, Rong FG, Barth RF, Codogni IM, Wilson JG (1998) The chemistry of neutron capture therapy. Chem Rev 98:1515
Telgmann L, Sperling M, Karst U (2013) Determination of gadolinium-based MRI contrast agents in biological and environmental samples: a review. Anal Chim Acta 764:1–16
Tokumitsu H, Ichikawa H, Fukumori Y (1999) Chitosan-gadopentetic acid complex nanoparticles for gadolinium neutron-capture therapy of cancer: preparation by novel emulsion-droplet coalescence technique and characterization. Pharm Res 161:830–1835
Truillet C, Bouziotis P, Tsoukalas C, Brugière J, Martini M, Sancey L, Brichart T, Denat F, Boschetti F, Darbost U, Bonnamour I, Stellas D, Anagnostopoulos CD, Koutoulidis V, Moulopoulos LA, Perriat P, Lux F, Tillement O (2015) Ultrasmall particles for Gd-MRI and (68) Ga-PET dual imaging. Contrast Media Mol Imaging 10:309–319
Wang S, Blaha C, Santos R, Huynh T, Hayes TR, Beckford-Vera DR, Blecha JE, Hong AS, Fogarty M, Hope TA, Raleigh DR, Wilson DM, Evans MJ, VanBrocklin HF, Ozawa T, Flavell RR (2019) Synthesis and initial biological evaluation of boron-containing prostate-specific membrane antigen ligands for treatment of prostate cancer using boron neutron capture therapy. Mol Pharm 16:3831–3841
Wang S, Zhang Z, Miao L, Li Y (2022) Boron neutron capture therapy: current status and challenges. Front Oncol 12:788770
Youle RJ, Strasser A (2008) The BCL-2 protein family: opposing activities that mediate cell death. Nat Rev Mol Cell Biol 9:47–59
Zhang Z, Chong Y, Liu Y, Pan J, Huang C, Sun Q, Liu Z, Zhu X, Shao Y, Jin C, Liu T (2023) A review of planned, ongoing clinical studies and recent development of BNCT in Mainland of China. Cancers (Basel) 15:4060